Vascular Pharmacology 116 (2019) 24–35

Contents lists available at ScienceDirect

Vascular Pharmacology

journal homepage: www.elsevier.com/locate/vph

MicroRNA-221-3p promotes pulmonary artery smooth muscle cells proliferation by targeting AXIN2 during pulmonary arterial hypertension

Xiaowei Nie[a,b,c,*], Yuan Chen[c], Jianxin Tan[a], Youai Dai[a], Wenjun Mao[c], Guowei Qin[d], Shugao Ye[c], Jie Sun[a,b], Zhenkun Yang[a,b], Jingyu Chen[a,b,c,*]

[a] Jiangsu Key Laboratory of Organ Transplantation, Wuxi People's Hospital Affiliated to Nanjing Medical University, PR China
[b] Center of Clincical Research, Wuxi People's Hospital of Nanjing Medical University, PR China
[c] Lung Transplant Group, Wuxi People's Hospital Affiliated to Nanjing Medical University, PR China
[d] Department of Anesthesiology, Wuxi People's Hospital Affiliated to Nanjing Medical University, PR China

ARTICLE INFO

Keywords:
Pulmonary arterial smooth muscle cells
Hypoxia
microRNA-221-3p
Axis inhibition protein 2
β-Catenin

ABSTRACT

Pulmonary arterial hypertension (PAH) is a pathological condition characterized by excessive cell proliferation and migration of pulmonary arterial smooth muscle cells (PASMC). PAH pathogenesis shares similarities with cancers such as excessive cell proliferation and apoptosis resistance. A previous study by our group revealed that decreased expression of a tumor suppressor-AXIN2 (Axis inhibition protein 2) was responsible for enhanced PASMC proliferation and suppressed apoptosis. Nevertheless, the mechanisms that regulate the downregulation of AXIN2 in PAH remain elusive. Data from the present study demonstrated that miR-221-3p acts as an upstream regulator of AXIN2 and functions to induce PASMC proliferation. We first showed that miR-221-3p expression was elevated in lung tissue and PASMC of PAH patients as well as in animal models of PAH. Human PASMC were transfected with a miR-221-3p mimic and miR-221-3p inhibitor, respectively, and their effects on the proliferation and migration was assessed using BrdU incorporation, PCNA staining and wound healing assays. In addition, we investigated the molecular mechanism through which miR-221-3p contributes to cell proliferation in PASMC and identified AXIN2 as a direct target gene of miR-221-3p by dual luciferase reporter gene assays, qRT-qPCR and western blotting. Furthermore, we found that ectopic expression of AXIN2 or pharmacological inhibition of β-catenin by XAV-939 can attenuate the effect of miR-221-3p on cell proliferation in PASMC. Moreover, intravenous injection of miR-221-3p inhibitor attenuated the progression of SU5416-hypoxia-induced PAH in rats. The results of the present study identified a new regulatory axis in which miR-221-3p and AXIN2 regulate the proliferation of PASMC.

1. Introduction

Chronic hypoxia-induced pulmonary arterial hypertension (PAH) is characterized by pulmonary arterial pressure due to pulmonary vasoconstriction and vascular remodeling, accompanied by right ventricular hypertrophy (RVH) and subsequent heart failure [1]. It is well accepted that the primary cellular mechanism underlying vascular remodeling is manifested by excessive proliferation and migration of pulmonary arterial smooth muscle cells (PASMC) [2] [3]. However, the exact molecular mechanisms that regulate PASMC proliferation and migration are incompletely understood.

Currently, a novel cancer-like concept for PAH has emerged. Disruption of major regulators of cancer, such as oncoproteins, tumor suppressors, and miRNAs are implicated as important factors in the pathogenesis of PAH. We have showed that decreased expression of a tumor suppressor-AXIN2 (Axis inhibition protein 2) was responsible for enhanced PASMC proliferation and suppressed apoptosis [4]. Nevertheless, the mechanisms that regulate this downregulation in PAH remain elusive.

MicroRNAs (miRNAs), a class of noncoding RNAs, that negatively

Abbreviations: PAH, pulmonary arterial hypertension; SD rats, Sprague-Dawley rats; miRNA, microRNA; mRNA, messenger RNA; AXIN2, Axis inhibition protein 2; RVSP, right ventricular systolic pressure; RVH, right ventricular hypertrophy; qRT-PCR, quantitative real-time polymerase chain reaction; PAEC, pulmonary artery endothelial cells; PASMC, pulmonary artery smooth muscle cells; PAs, pulmonary arteries; SU-5416, Semaxanib; WT, wild type; MTT, 3-(4, 5-dimethyl-2-thiazolyl)-2, 5-diphenyl-2-H-tetrazolium bromide; Mut, mutant; NC, negative oligonucleotide; KO, knockout; VSMC, vascular smooth muscle cells; PTEN, phosphatase and tensin homolog; siRNA, small interfering RNA; siAXIN2, knockdown of AXIN2 by small interfering RNA; BrdU, 5-Bromo-2-deoxyUridine; PCNA, proliferating cell nuclear antigen; DMEM, dulbecco minimum essential medium; GSK3β, glycogen synthase kinase 3β

* Corresponding authors at: Jiangsu Key Laboratory of Organ Transplantation, Wuxi People's Hospital Affiliated to Nanjing Medical University, No. 299, Qing Yang Road, Wuxi, Jiangsu 214021, PR China.
E-mail addresses: niexiaowei@njmu.edu.cn (X. Nie), cjy_wx@163.com (J. Chen).

http://dx.doi.org/10.1016/j.vph.2017.07.002
Received 25 December 2016; Received in revised form 13 May 2017; Accepted 6 July 2017
Available online 08 July 2017

regulate gene expression by degradation or translational inhibition of microRNA target genes, acting as posttranscriptional regulators to fine-tune protein synthesis [5,6]. miRNAs have been identified as essential modulators of a variety of genes and cellular processes including cell proliferation, apoptosis, migration and differentiation [7,8]. Several miRNAs have been reported to regulate different steps in the process of angiogenesis and vascular remodeling [9]. In cancer, AXIN2 expression is regulated by microRNA-221-3p (miR-221-3p) according to TargetScan 6.2, AXIN2 is in fact a predicted target of miR-221-3p. miR-221-3p has been recognized as a tumor-suppressor that reported to regulate physiological and pathological vascular processes such as angiogenesis [10] and neointimal formation [11]. miR-221 was reported to be markedly up-regulated in vascular smooth muscle cells (VSMC) in response to vascular injury and in proliferative VSMC [12]. miR-221 has shown to be critical for the PDGF-dependent promotion of cell migration and growth in VSMC [19,20]. miR-221 also negatively regulates a tumor suppressor-phosphatase and tensin homolog (PTEN), resulting in increased expression of proinflammatory mediators and activates proliferation, migration, and hypertrophy of VSMC [18]. Hence, miR-221-3p upregulation is associated with proliferative and inflammatory disorders, both crucial pathomechanisms of PAH development. We thus hypothesized that increased miR-221-3p expression in PAH leads to AXIN2 downregulation promoting the proliferation/apoptosis imbalance of PAH-PASMC and thus triggers PAH development.

Using a multidisciplinary and translational approach, we demonstrated in human PAH lungs, distal PAs, and PASMC that miR-221-3p is upregulated. This downregulation accounts for AXIN2 upregulation, promoting PAH-PASMC proliferation and resistance to apoptosis. Finally, in vivo, downregulation of miR-221-3p using intravenous injection of miR-221-3p inhibitor improves SU-5416/hypoxia-PAH in rats.

2. Materials and methods

2.1. Materials

Antibodies against AXIN2, β-catenin, proliferating cell nuclear antigen (PCNA) (ab29), cyclin A (ab206746), cyclin D (ab40754), cyclin E (ab89585), β-actin (ab8229) were from Abcam Co.LTD (Cambridge, MA, USA). Alpha smooth muscle actin (α-SMA) was purchased from RD Systems, Inc. (Minneapolis, MN, USA). Enhanced chemiluminesence (ECL) reagents were from Amersham International (Amersham Biosciences, Freiburg, Germany). Sugen 5416 were purchased from Sigma-Aldrich (St. Louis, MO, USA). Cell Counting Kit-8 was purchased from Dojindo Laboratories (Dojindo, Kumamoto, Japan). BrdU cell proliferation assay kit was from Cell Signaling Technology, Inc. (Danvers, MA, USA). All reagents for cell cultures were purchased from Invitrogen Life Technologies, Inc. (Burlington, Canada).

2.2. Patients and clinical samples collection

This study was approved by the Ethics Committee of Nanjing Medical University affiliated Wuxi People's Hospital (Permit Number: 2015-02-21-36), which was in accordance with The Code of Ethics of the World Medical Association (Declaration of Helsinki) for experiments involving humans. Each individual provided written informed consent. 10 preoperative lung tissue samples of PAH patients (the majority of which were female, average age was 45 ± 8 years, mean pulmonary artery pressure was 87 ± 15 mm Hg) and 10 matched healthy control samples were collected at the Lung Transplant Group, Wuxi People's Hospital Affiliated of Nanjing Medical University (Wuxi, China) [13,14]. Human PAH specimens were collected from patients undergoing lung transplantation; paired healthy controls were collected from the unused donor control subjects (Table 1). Lung tissues were immediately transferred into chilled oxygenated Krebs solution (in mM: KCl 4.2, $CaCl_2$ 2.5, NaCl 116, NaH^2PO_4 1.6, $MgSO_4$ 1.2, D-glucose 11 and $NaHCO_3$ 22, pH 7.4). Primary human PASMC and PAEC were isolated from PAs dissected from both control and PAH lungs of human under microscope using a previously described method [15]. Briefly, human PAs were minced and digested in Hanks' balanced salt solution containing typeII collagenase and DNase. Upon the removal of the PAEC, the remaining smooth muscle was digested with 1.5 mg/mL collagenase, 0.5 mg/mL elastase, and 1.5 mg/mL BSA at 37 °C to make a suspension of PASMC. The single PASMC was resuspended in DMEM containing 10% fetal bovine serum (FBS) and 100 μg/mL penicillin, 100 IU/mL streptomycin and incubated in a humidified atmosphere of 5% CO_2 in air at 37 °C for 1 week. The PASMC were confirmed by staining for α-SMA. Cell viability (usually > 98%) was determined by Trypan Blue exclusion. Cells were used at passages 3–8. In vitro experiments were performed in primary human PASMC (PromoCell, C-12521, Heidelberg, Germany) and PAEC (PAEC, ScienCell, 3100, Santiago City, CA, USA) obtained commercially. To induce hypoxia, cells were placed into a hypoxia chamber with an atmosphere of 5% CO_2/92% N_2 with an oxygen level of 3% for the indicated time intervals [16].

Table 1
Characteristics of PAH patients and control unused donors.

Patient ID	Age, y	Sex	Race	Diagnosis/cause of death	PAP(S/D/M) (mm Hg)
PAH-01	51	M	Yellow	HPAH	89/42/62
PAH-02	53	M	Yellow	HPAH	92/40/63
PAH-03	50	F	Yellow	HPAH	87/48/60
PAH-04	48	M	Yellow	HPAH	114/78/90
PAH-05	42	M	Yellow	HPAH	81/55/67
PAH-06	40	M	Yellow	HPAH	120/68/85
PAH-07	41	M	Yellow	HPAH	106/60/75
PAH-08	49	M	Yellow	HPAH	98/47/61
PAH-09	37	M	Yellow	HPAH	125/80/95
PAH-10	45	F	Yellow	HPAH	110/65/80
Control-01	49	M	Yellow	Intracranial hemorrhage	N/A
Control-02	40	M	Yellow	Anoxia of brain	N/A
Control-03	51	F	Yellow	Anoxia of brain	N/A
Control-04	53	M	Yellow	Subarachnoid hemorrhage	N/A
Control-05	44	M	Yellow	Anoxia of brain	N/A
Control-06	46	M	Yellow	Cerebrovascular/stroke	N/A
Control-07	52	M	Yellow	Acute myocardial infarction	N/A
Control-08	40	M	Yellow	Anoxia of brain	N/A
Control-09	39	M	Yellow	Anoxia of brain	N/A
Control-10	42	F	Yellow	Anoxia of brain	N/A

Definition of abbreviations: ID = identification; N/A = data not available; PAH = pulmonary arterial hypertension; PAP (S/D/M), pulmonary artery pressure (systolic/diastolic/mean); HPAH, hypoxic pulmonary arterial hypertension; PAP, pulmonary artery pressure (mm Hg); M, male; F, femal; N/A, data not available. Hemodynamic data were obtained from catheterization study performed closest to transplantation.

2.3. Animal models

Adult male Sprague-Dawley (SD) rats with a mean weight of 160–200 g were from Slack laboratory animal in Shanghai, which is fully accredited by the Institutional Animal Care and Use Committee (IACUC). For the SU-5416/hypoxia model, rats were injected with the vascular endothelial growth factor Flk-1/KDR receptor inhibitor Semaxanib (SU-5416, 20 mg/kg) once weekly and put in hypoxia (10% O_2) for 3 weeks. Control rats were injected with the same volume of vehicle alone. After 3 weeks of hypoxia and weekly injections of SU-5416 or vehicle, animals were either studied and euthanized or returned to normoxia for an additional 2 weeks [17]. SU-5416/hypoxia rats were injected weekly with either scrambled control or miR-221-3p inhibitor lentivirus or knockdown of AXIN2 by small interfering RNA (siAXIN2) lentivirus (4×10^8 TU) for 3 weeks. Oxygen concentration

was maintained at 10% by controlling the flow rates of compressed air and N_2. Concentrations of O_2 and CO_2 in chamber were checked daily. Normoxic animals were kept at 21% O_2 in the same room adjacent to the hypoxic chamber [18]. Rats were kept in a room with12-hour light/dark exposure cycles. Animals were age and body weight matched. All animal experiments were in full compliance with the Guide for the Care and Use of Laboratory Animals published by the US National Institutes of Health (NIH Publication No. 85-23, revised 1996) and approved by Nanjing Medical University. PASMC and PAEC were isolated from rats with PAH using methods as previously described [15].

2.4. Measurement of right ventricular hypertrophy index

The ventricles and ventricular septum were removed, weighed and dehydrated for 24 h at 60 °C. Then a ratio of right to left ventricle plus interventricular septum weight (RV/LV + S) was calculated for determination of right ventricular hypertrophy [19].

2.5. Histological staining & morphological analysis

The distal part of the lungs from patients and rats as described above were removed and fixed in 4% paraformaldehyde for overnight fixation, embedded in paraffin, serially sectioned at 5-μm and stained with hematoxylin and eosin. Lung morphology was visualized using an Olympus BX-51 microscope (Olympus, Tokyo, Japan) with a Retiga 4000RV camera (QImaging, Vancouver, Canada). The percentage of pulmonary artery wall thickness and arterial radii of the 51- to 150-μm (outer diameter) pulmonary arteries (PAs) were measured using Image Pro Plus 6.0 software (MediaCybernetics, Rockville, MD, USA) [20].

2.6. Immunohistochemistry

Lung tissue sections (5 μm) were incubated with primary antibody against α-SMA in 2% bovine serum albumin (BSA) in PBS at a dilution of 1:200 at 4 °C overnight. Slides were washed three times in PBS before incubation for corresponding secondary antibody [21]. Negative control immunostainings were performed with the omission of primary antibodies. Statistical significance was assessed by comparing the percentage of muscularized vessels between groups. Assessment of muscularization was performed in a blinded fashion. Alternatively, immunofluorescent assessment of rat lung sections was performed using mouse anti-α-SMA at 1:200 in 5% goat serum, followed by Alexa Fluor 488 or 594 conjugated anti-mouse secondary IgG.

2.7. Measurement of right ventricular systolic pressure (RVSP)

Right heart catheterization was used to estimate RVSP according to Song Y [22]. Before catheterization, rats were anesthetized with 45 mg/kg pentobarbital sodium by intraperitoneal injections. A pressure-sensing catheter was inserted from the right jugular vein and advanced into the right ventricle and the pressures were recorded. RVSP was continuously recorded for 45 min.

2.8. Real-time RT-PCR and microRNA analysis

Total RNA was isolated from cultured cells or lung tissue samples using the Trizol Reagent according to the manufacturer's instructions. The purity and concentration of RNA was determined using NanoDrop 1000 spectrophotometer (Thermo Scientific, Wilmington, MA). After DNase I treatment, reverse transcription for mRNA was carried out using the High Capacity cDNA reverse transcription kit (Applied Biosystems, Foster City, CA, USA). MicroRNA was extracted using mirVana miRNA Isolation Kits (Applied Biosystems, Foster City, CA, USA) according to the manufacturer's protocol. RNA reverse transcription was performed with the ABI TaqMan microRNA reverse transcription kit using specific stem-loop primers. Quantification of expression levels of miR-221-3p was determined by quantitative real time-PCR using SYBR Green and an Applied Biosystems 7500 detection system (Foster City, CA, USA). U6 small nuclear RNA (U6 snRNA) and RNU48 were used for normalization, and all reactions were run in triplicate. Specific PCR amplification was confirmed by performing dissociation curve analysis [23]. The cycle threshold (C_T) value was calculated. Sequences of miR-221-3p, stem-loop primers, and primers for real time RT-PCR are as follows: miR-221-3p: mature sequence: AGCUACAUUGUCUGCUGGGUUUC; forward primer: 5′-CCCAGCATTTCTGACTGTTG-3′ and antisense: 5′-TGTGAGACCATTTGGGTGAA-3′. U6 snRNA: forward primer: 5′-CTCGCTTCGGCAGCACA-3′ and reverse primer: 5′-AACGCTTCACGAATTTGCGT-3′. RNU48: forward primer: 5′-TGATGATGACCCCAGGTAACTCT-3′ and reverse primer: 5′-GCGAGCACAGAATTAATACGAC-3′. AXIN2: forward primer: 5′- CTGGCAACTCAGTAACAGCC-3′ and reverse primer: 5′- GCCTGGTGTTGGAAGAGACA-3′. β-Catenin: forward primer: 5′- CATCTCGCCATGCTATTA-3′ and reverse primer: 5′- AAGGTGGAGTCCTAAAGC-3′. GAPDH: forward primer: 5′-GGGAAGCTT GTCATCAATGGA-3′ and reverse primer: 5′-TCTCGCTCCTGGAAGATG GT–3′.

2.9. Knockdown or ectopic expression of miR-221-3p

The miR-221-3p expression was knocked down by transfection of miR-221-3p inhibitor or induced by miR-221-3p mimic. miR-221-3p mimic (5′-AGCUACAUUGUCUGCUGGGUUUC-3′) or inhibitor (5′-GAAACCCAGCAGACAAUGUAGCU-3′) and *Caenorhabditis elegans* miR-67 (cel-miR-67 mature sequence: UCACAACCUCCUAGAAAGAGUAGA, which lacks homologs in mammals and was used as a negative oligonucleotide) were purchased from RiboBio (Guangzhou, China). Cel-miR-67 was used as the negative oligonucleotide (NC) for miRNA inhibitor and mimic. The cells were seeded in 96/24-well plates, then transfected with 40 nM inhibitors or mimics with Lipofectamine 2000 (Invitrogen, Burlington, Canada) for 24 h. The transfection efficiency was assessed using fluorescence microscopy via carboxyl fluorescein labelled miRNA. Cells were subjected to RNA/protein extraction or for further assays after transfection [24].

2.10. Lentivirus vector construction

To generate lentivirus-mediated silencing vector, small interfering (5′-ACCACCACTACATCCACCA-3′) sequence targeting human AXIN2 and scrambled control RNA (5′-TTCTCCGAACGTGTCACGT-3′) were cloned into the lentivirus knockdown vector. Lentiviral vector construction and vector packaging were carried out as previously described [25]. A number of 3×10^6 293T cells were seeded in a T25 flask. A lentiviral vector and packaging vectors were co-transfected into 293T cells. After 6 h transfection, the co-transfection solution was replaced by complete DMEM medium. The packaged recombinant lentiviruses were harvested from the supernatant of cell cultures in 72 h after transfection and mixed with polybrene (8 μg/mL). Starting 72 h post-infection, infected cells were then selected with 5 μg/mL puromycin for about 2 weeks to generate the stable transfectants. New media containing fresh puromycin were replaced every 3 days until the generation of resistant colonies. AXIN2 protein levels were assessed by western blot analysis three days after lentiviral transduction.

2.11. BrdU cell proliferation assay

To assess the proliferation rate, 5-Bromo-2-deoxyUridine (BrdU) assay was performed. PASMC were seeded into 96-well plates. Cells were transfected with 40 nM of miR-221-3p inhibitor/miR-221-3p mimic for 24 h using Lipofectamine 2000. After 48 h, 10 μL BrdU was added to each well and incubated for an additional 4 h. The cells were then fixed, and incubated with BrdU antibody for 1 h. Cells were washed for three times and incubated with 200 μL substrate solution for 5 to 30 min and 25 μL of 1 M H_2SO_4 was added. Finally, absorbance at

450 nm was measured using an enzyme-linked immunosorbent assay reader (Thermo Scientific, Waltham, MA). The measured absorbance directly correlates with the proliferation of cells.

2.12. Prediction of miRNAs targeting AXIN2

The miRNA target predicting algorithms miRDB (http://mirdb.org/miRDB/), TargetScan (http://www.targetscan.org/), and PicTar (http://pictar.mdcberlin.de/) were used to predict miRNAs targeting AXIN2 and the binding regions.

2.13. Luciferase assay

The Axin2 3'UTRs containing predicted miR-221-3p binding sites were inserted into pMIR-REPORT luciferase reporter vectors (Ambion Austin, TX, USA) after amplification from human genomic DNA using primers, and to obtain constructs containing wild-type Axin2 3′-UTR (WT-3′-UTR), Axin2-MUT contained sequences with mutations in the first putative binding site of Axin2 3′-UTR (Mut-3′-UTR). Predicted seed regions in these mRNA sequences were created, using primers including mutated sequences. Recombination constructs, pRL-TK (Promega, Madison, WI, USA) and miR-221-3p were co-transfected into PASMC using lipofectamine 2000. Plasmids of pRL-TK containing Renilla luciferase were used as internal control. Firefly and Renilla luciferase activity were measured using the Dual-Luciferase Reporter assay system (Promega Corp, Madison, WI, USA) according to the manufacturer's instructions after 24 h transfection. All transfection assays were repeated in triplicate in three independent experiments [26,27].

2.14. Enzyme-linked immunosorbent assay

For immunosorbent assay, whole-cell lysates were prepared with radioimmnoprecipitation assay buffer (Thermo Scientific, Massachusetts, USA). A cell-based enzyme-linked immunosorbent assay (ELISA) (R & D Systems, MN, USA) that measures total AXIN2 protein in the context of whole cells was used to quantify AXIN2 protein levels [28].

2.15. Western blotting

Cells transfected with miR-221-3p mimic or miR-221-3p inhibitor, siAXIN2 or control lentvirus were rinsed with PBS and mechanically harvested into cell lysis buffer (Beyotime Biotechnology, Beijing, China), subjected for sonication and centrifugation. Supernatants were collected and protein concentration determined using the Bio-rad DC Assay kit (Hercules, CA, USA). 50 μg of total protein was fractionated by 10% of SDS-PAGE and electroblotted onto a PVDF-membrane. Antibodies used for immunoblotting were: anti-AXIN2, anti-β-catenin, anti-PCNA, anti-Cyclin A, anti-Cyclin D, anti-Cyclin E and anti-β-actin. For detection of proteins, horseradish peroxidase (HRP)-conjugated anti-rabbit and anti-mouse antibodies (1:5000) were incubated for 1 h at room temperature before performing an enhanced chemiluminescence reaction and subsequent exposure to X-ray film (Thermo Scientific, Massachusetts, USA). Evaluation for PCNA and Cyclin D, Cyclin A and Cyclin E was obtained from the same gel after striping (30 min at 50 °C). Evaluation for AXIN2 and β-catenin after siAXIN2 was obtained from the same gel after striping [29].

2.16. Cell viability

Cell viability was measured by Cell Counting Kit 8 (CCK-8, Dojindo Tokyo, Japan). After treatment with miR-221-3p mimic and miR-221-3p inhibitor for 48 h, PASMC were seeded on 96-well plates at a density of 4×10^4 cells per well and then exposed to normoxia or 48 h hypoxia in presence with AXIN2 or XAV-939, which were added every 24 h under hypoxic conditions. The cell viability of cultured PASMC was examined using CCK-8. CCK-8 (10 μL) was added to each well with treated cells and incubated at 37 °C for another 4 h. The absorbance was read at 450 nm using a microplate reader (Thermo Scientific, Waltham, MA, USA). All experiments were performed in quintuplicate and repeated thrice.

2.17. MTT cell proliferation assay

Human PASMC was seeded at a density of 4×10^3 cells per well in 96-well plates followed by 24 h incubation in serum-free DMEM, and then exposed to miR-221-3p inhibitor/miR-221-3p mimic for 48 h. MTT (0.25 mg/mL) was added to each well. After 4 h incubation at 37 °C, the supernatant was carefully removed, and then 150 μL of DMSO was added to each well. The absorbance at 450 nm was measured with an enzyme-linked immunosorbent assay reader (Thermo Scientific, Waltham, MA, USA). Six replicated wells were included in each group, and means were calculated. All determinations were confirmed in at least three independent experiments [30].

2.18. Immunofluorescence

PASMC were plated in 24-well chamber slides at a density of 1×10^4 cells per well. Cells were starved for 24 h and then treated with miR-221-3p inhibitor/miR-221-3p mimic for 48 h under normoxic (21% O_2) and hypoxic (3% O_2) conditions. After treatment, cells were fixed with 4% paraformaldehyde for 15 min at room temperature and stained with anti-PCNA, anti-AXIN2, anti-β-catenin antibodies overnight at 4 °C. Alexa Fluor 488 conjugated anti-mouse IgG were used as secondary antibodies. Images (3–5 non-overlapping randomly selected fields for each slide) were taken using a laser scanning confocal microscope (Leica, Heidelberg, Germany). DAPI was used to counterstain nuclei. Percentages of cells nuclei positive for PCNA, AXIN2, β-catenin were determined.

2.19. Cell migration assay

For wound healing assays, a confluent layer of cells transfected with control or miR-221-3p inhibitor/miR-221-3p mimic for 48 h was wounded using The Cell Comb™ scratch assay (Millipore, CA, USA) before fresh culture media containing 2 μm hydroxyurea (Sigma) was added to block cell proliferation. Migration was assessed at 24 h with addition of Calcein-AM (Invitrogen; final concentration of 0.5 g/mL). After incubation for 15 min at 37 °C, images were captured using confocal microscopy, and the migrated distance was measured at 20 points along the wound edge using Image J software (http://imagej.nih.gov/ij/), as described previously [31]. Assessment of wound healing was performed in a blinded fashion.

2.20. Statistical analysis

Results are presented as mean ± SEM. Statistical analysis was performed with the Prism software package (San Diego, CA, USA). Comparisons between two groups were made using Student's *t*-test while three or more groups were determined by ANOVA when appropriate, followed by the Student-Newman-Keuls post-hoc analysis. Only a sample size ≥ 5 was subjected to statistical analysis. A p value < 0.05 was considered statistically significant ($^*p < 0.05$, $^{**}p < 0.01$, $^{***}p < 0.001$).

3. Results

3.1. miR-221-3p was up-regulated in lung tissue and PASMC from rats and human with PAH

We investigated the expression levels of miR-221-3p in lung tissue samples of PAH patients. The morphology of PAs from PAH patients

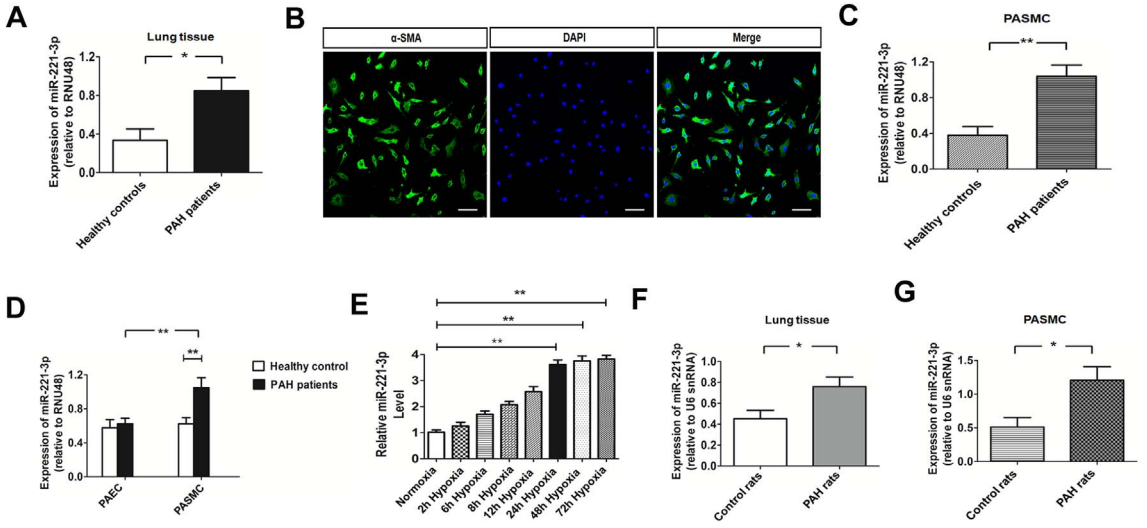

Fig. 1. Expression of miR-221-3p in patients with PAH and rats with SU-5416/hypoxia-induced PAH.
A, Expression of miR-221-3p in lung tissues from patients with PAH relative to RNU48. **B**, Identification of PASMC from PAs of PAH patients. **C**, Levels of miR-221-3p in PASMC isolated from PAs of PAH patients. **D**, Comparison of miR-221-3p expression levels between PASMC and PAEC from PAs of PAH patients. **E**, Expression of miR-221-3p in PASMC exposed to hypoxia for the indicated time intervals. **F**, Expression of miR-221-3p in lung tissues from SU-5416/hypoxia rats. **G**, Levels of miR-221-3p in PASMC isolated from SU-5416/hypoxia rats. Bars indicate mean ± SEM. n = 10.*p < 0.05, **p < 0.01 in comparison with respective control. PAH, pulmonary arterial hypertension; miR-221-3p, microRNA-221-3p; PAs, pulmonary arteries; PASMC, pulmonary artery smooth muscle cells; PAEC, pulmonary artery endothelial cells.

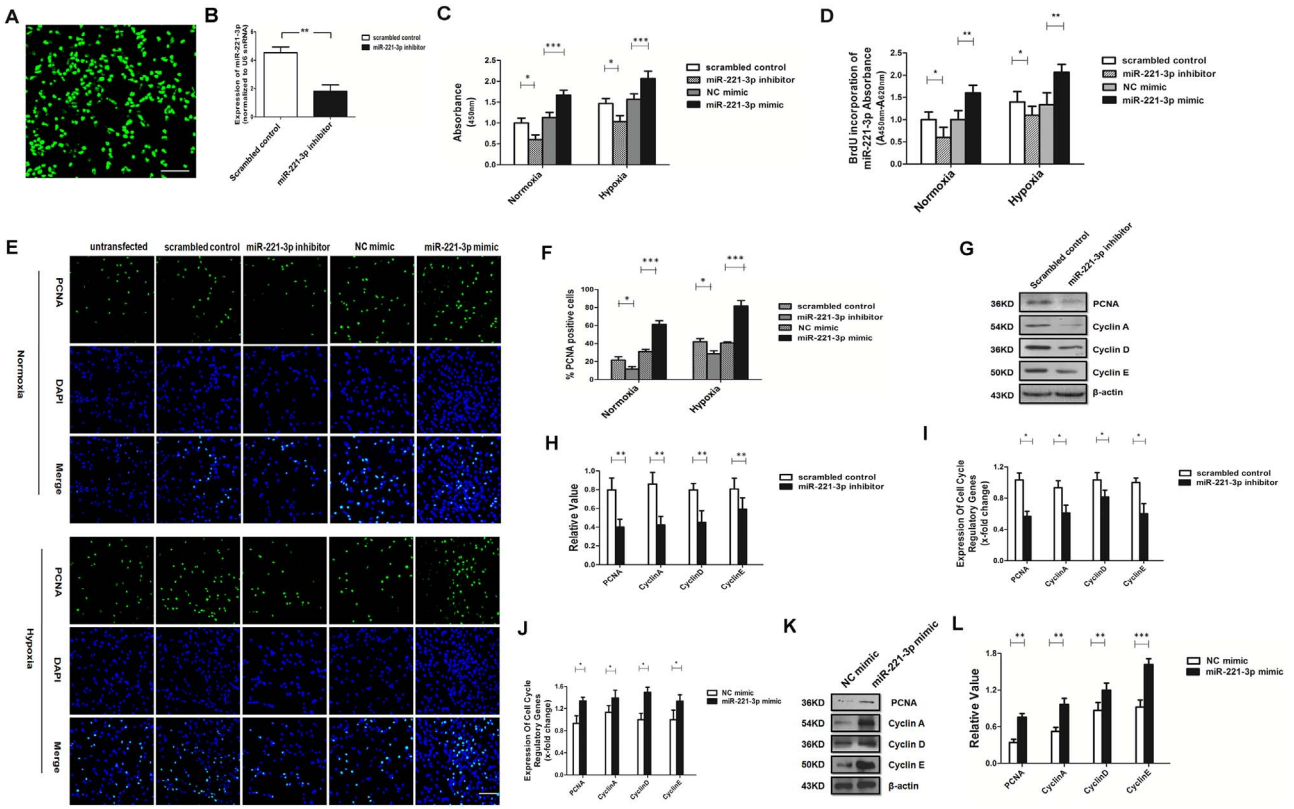

Fig. 2. miR-221-3p regulates PASMC proliferation and modulates the expression of cyclin-dependent genes.
A, Fluorescence microscopy of PASMC transfected with the fluorescence control demonstrated that transfection efficiency was high. Scale bars are 50 μm. **B**, miR-221-3p expression levels were analyzed in PASMC transfected with scrambled control or miR-221-3p inhibitor (n = 6). **C**, Cell viability were analyzed in PASMC transfected with scrambled control, miR-221-3p inhibitor, NC or miR-221-3p mimic and then exposed to normoxia or hypoxia for 24 h (n = 3). **D**, BrdU incorporation assay was used to determine the proliferation of PASMC transfected with miR-221-3p mimic and miR-221-3p inhibitor under normoxia or hypoxia (n = 6). **E**, Immunohistochemical staining against PCNA were used to determine the effects of miR-221-3p expression alteration on cell proliferation. Scale bars are 50 μm. **F**, The percentage of PCNA positive cells were calculated (n = 5). **G**, Representative images of six experiments are shown PCNA, cyclin A, cyclin D and cyclin E protein expression levels in PASMC transfected with scrambled control or miR-221-3p inhibitor. **H**, Densitometric analysis of the immunoblot data (n = 6). **I**, The expression level of PCNA, cyclin A, cyclin D and cyclin E mRNA in PASMC transfected with scrambled control or miR-221-3p inhibitor (n = 6). **J**, The expression level of PCNA, cyclin A, cyclin D and cyclin E mRNA in PASMC transfected with control mimic or miR-221-3p mimic (n = 6). **K**, Representative images of six experiments are shown PCNA, cyclin A, cyclin D and cyclin E protein expression levels in PASMC transfected with NC or miR-221-3p mimic. **L**, Densitometric analysis of the immunoblot data (n = 6). *p < 0.05, **p < 0.01, ***p < 0.001 compared to NC control or scrambled control. Bars indicate mean ± SEM. miR-221-3p, microRNA-221-3p; NC, negative oligonucleotide; BrdU, Bromodeoxyuridine; qPCR, real-time quantitative PCR; PASMC, pulmonary artery smooth muscle cells; PCNA, proliferating cell nuclear antigen.

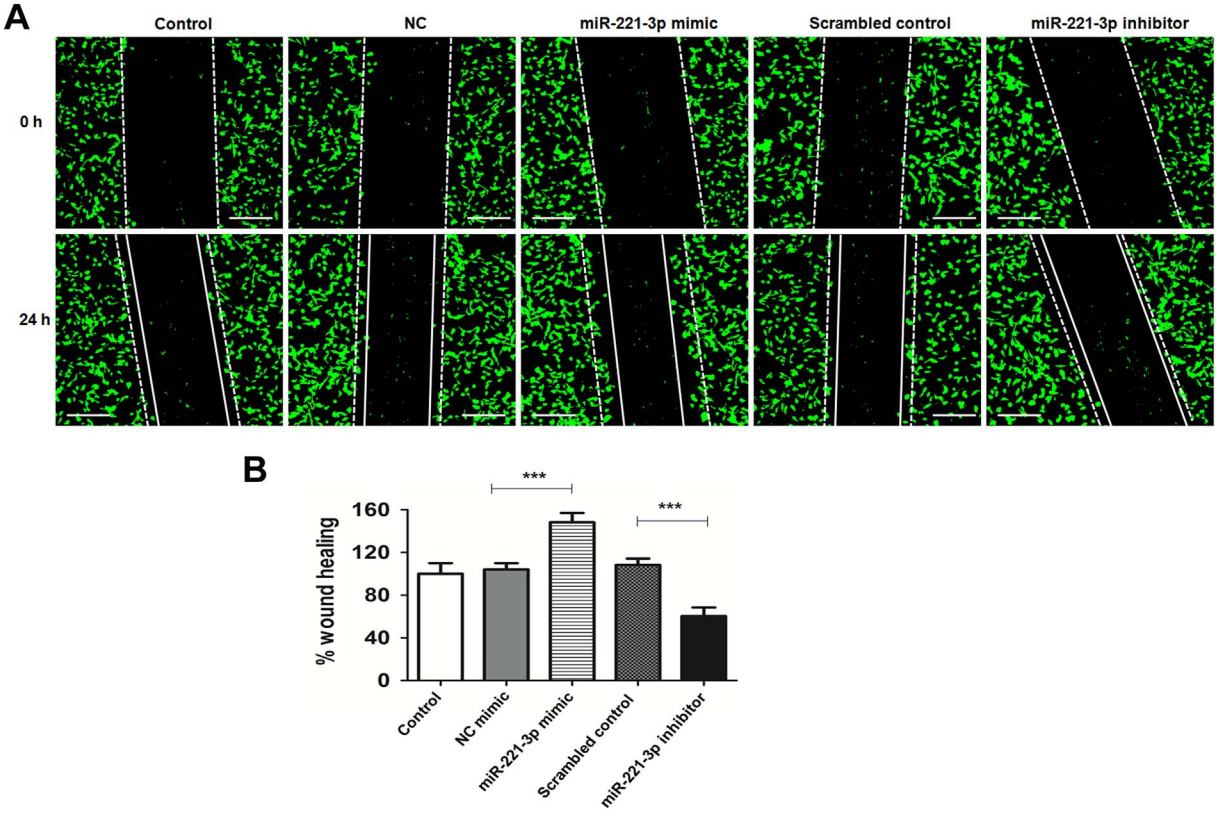

Fig. 3. miR-221-3p promotes migration of human PASMC.
A, Representative images of wound-healing assay showing migration of human PASMC either with miR-221-3p mimic or inhibitor. **B**, Bar chart showing relative decreased wound width after 24 h (n = 6). ***p < 0.001 compared to NC control or scrambled control. Bars indicate mean ± SEM. miR-221-3p, microRNA-221-3p; NC, negative oligonucleotide.

and healthy lung donors used were shown in **Fig. S1**. Expression levels of miR-221-3p were found to be significantly increased in PAH patients as compared to control (normalized to RNU48 snRNA. Fig. 1A). Furthermore, we examined miR-221-3p levels in PASMC isolated from PAH patients and normal controls. The purity of PASMC from PAH patients was evaluated by α-SMA immunohistochemical staining (Fig. 1B). miR-221-3p was significantly up-regulated in PASMC of patients with PAH as compared to healthy controls (Fig. 1C). Of note, miR-221-3p was shown to be comparatively higher in PASMC than PAEC of PAH patients (Fig. 1D). Hypoxia up-regulated the expression of miR-221-3p in PASMC (by 1.5-fold after 24 h of hypoxia, Fig. 1E).

We further investigated the expression of miR-221-3p in rat models of PAH. We isolated total lung and PASMC from SU-5416/hypoxia-PAH rats. The wall thickness and RVSP were increased by SU-5416 plus 21-day chronic hypoxia, demonstrating PAH and RV hypertrophy were successfully induced in SU-5416/hypoxia-PAH rats (**Fig. S2**). Expression levels of miR-221-3p were analyzed by qRT-PCR. miR-221-3p was found to be significantly up-regulated in lung tissue and PASMC of SU-5416/hypoxia rats as compared to controls (normalized to U6 snRNA. Fig. 1F–G).

3.2. Effect of miR-221-3p on PASMC proliferation and migration

To test whether miR-221-3p regulates cell proliferation and migration, BrdU incorporation, PCNA staining and wound healing assays were performed in PASMC transfected with miR-221-3p inhibitor/mimic. A miR-221-3p mimic and negative control (vector) were transfected into PASMC. A transfection efficiency of miR-221-3p mimic in PASMC was achieved following observation under a fluorescence microscope (Fig. 2A). As measured by qPCR, transfection of PASMC with miR-221-3p inhibitor significantly decreased the expression of miR-221-3p compared to scrambled controls (Fig. 2B). MTT assay showed cell viability of PASMC was increased by miR-221-3p mimic, and were decreased by miR-221-3p inhibitor (Fig. 2C). As presented in Fig. 2D, the proliferation rate of PASMC was significantly increased by miR-221-3p mimic when compared to control cells, and was decreased by miR-221-3p inhibitor under normoxia and hypoxia. PCNA staining further confirmed the proliferative effect of miR-221-3p mimic on PASMC (Fig. 2E, F). The protein and mRNA levels of the most abundantly cell cycle regulatory genes including PCNA, cyclin A, cyclin D and cyclin E, were found significantly decreased by miR-221-3p inhibitor (Fig. 2G–I). miR-221-3p mimic significantly increased protein and mRNA expression of PCNA, cyclin A, cyclin D and cyclin E (Fig. 2J–L). These data imply that miR-221-3p mimic induces proliferation of PASMC via up-regulation of cell cycle-related proteins. However, miR-221-3p has no effect on the proliferation of PAEC as showed in **Fig. S3**. As shown in Fig. 3A and B, the decrease in the width of the scratched wound was larger in miR-221-3p mimic transfected cells than in control cells after 24 h, and miR-221-3p inhibitor led to a slower decrease in wound healing compared with scrambled control transfection after 24 h. Taken together these data demonstrate that hypoxia-induced miR-221-3p increase can promote proliferation and migration of human PASMC.

3.3. Inhibition of miR-221-3p attenuates the development of PAH in rats

In order to determine the role of miR-221-3p in PAH development, the miR-221-3p inhibitor was transfected to the SU5416-hypoxia rats by endotracheal drip. The results showed a decrease of miR-221-3p level in lung tissue as well as in PASMC of rats after injection with miR-221-3p inhibitor compared to controls receiving vehicle (Fig. 4A and B). Then the RVSP, RVH were measured and analyzed. The RVSP in the group treated with miR-221-3p inhibitor was significantly decreased than that in the group treated with scrambled control ((44.66 ± 0.85) mm Hg vs (24.64 ± 0.76) mm Hg) (Fig. 4C), its RVH was significantly

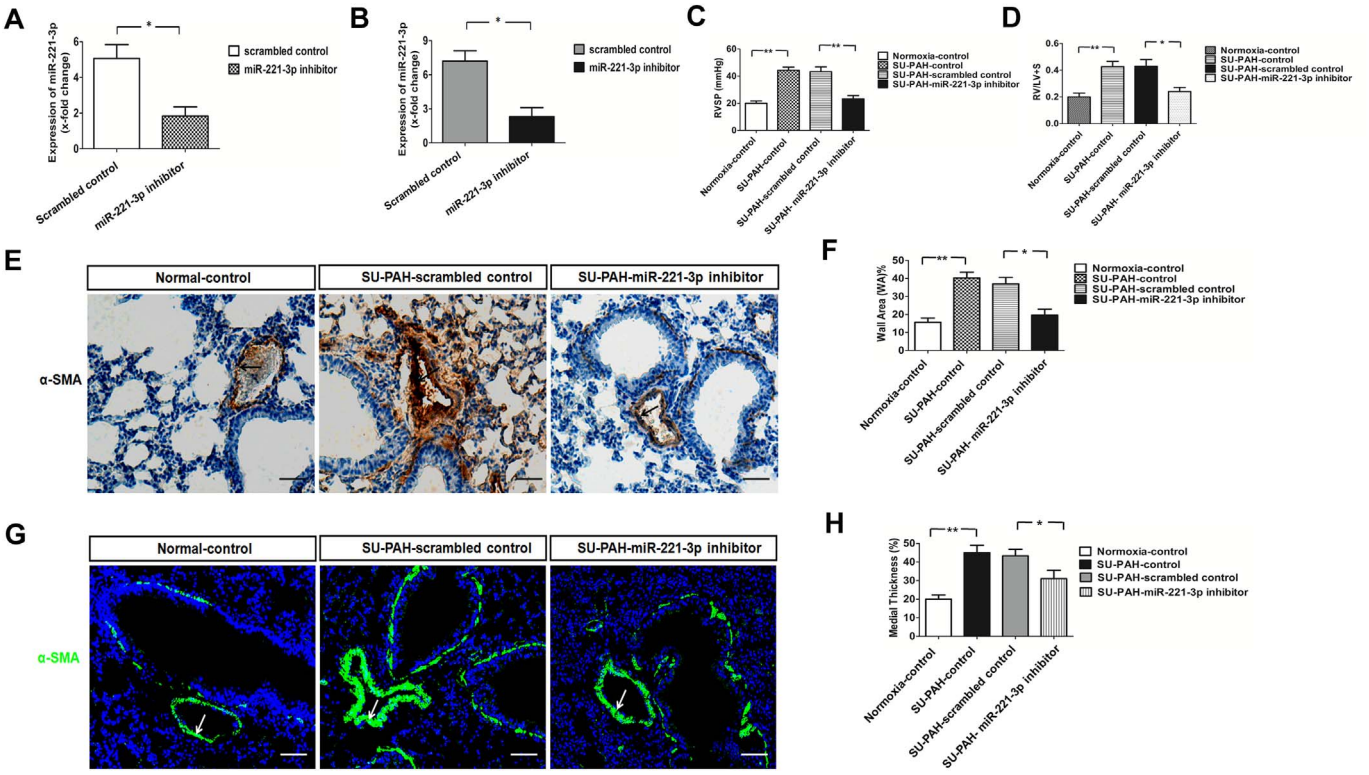

Fig. 4. miR-221-3p inhibitor transfection attenuated pulmonary vascular remodeling and pulmonary arterial hypertension in rats.
A, Expression of miR-221-3p in lung tissues taken from rats transfected with miR-221-3p inhibitor lentivirus (n = 4). **B**, Expression of miR-221-3p in PASMC isolated from rats transfected with miR-221-3p inhibitor lentivirus (n = 4). **C**, Assessment of RVSP in SU-5416/hypoxia rats and controls, or after 3 weeks of miR-221-3p inhibitor treatment of control or SU-5416/hypoxia rats (n = 6). **D**, Right ventricular hypertrophy in the same animals as in **C** (n = 6). **E**, Representative images of immunohistochemical staining for α-SMA in lung sections from control or SU-5416/hypoxia rats without or with miR-221-3p inhibitor treatment. Scale bars, 100 μm. **F**, The relative area of vascular wall WA% in the same animals as in **E** (n = 3). **G**, Immunofluorescent images of vessels stained with α-SMA from control or SU-5416/hypoxia rats without or with miR-221-3p inhibitor treatment (n = 6). Scale bars, 100 μm. **H**, Decreased percentage of wall thickness of pulmonary arteries in external diameter in SU-5416/hypoxia rats with miR-221-3p inhibitor treatment for 3 weeks compared with scrambled control-treated SU-5416/hypoxia rats. Arrows indicate positive staining around pulmonary vasculature. Bars indicate mean ± SEM. *p < 0.05, **p < 0.01 compared to scrambled control. miR-221-3p, microRNA-221-3p; RVSP, right ventricular systolic pressure; RV/(LV + S), right ventricular hypertrophy index; α-SMA, α-smooth muscle actin; WA, wall area.

decreased than that in control group (Fig. 4D). Furthermore, we carried out the immunohistochemical staining for α-SMA in order to demonstrate the medial hypertrophy of pulmonary vessels contributing to the pathogenesis of PAH. The results of the immunohistochemical staining of α-SMA in scrambled control and miR-221-3p inhibitor treated rats after the induction of PAH are presented in Fig. 4E, which depicts the α-SMA staining in a normal vessel in control rats under normoxia. There was deep staining of α-SMA in PAH rats indicating obviously thickening of the pulmonary vessels. However, these changes were blunted by miR-221-3p inhibitor (Fig. 4F). SU5416-hypoxia rats transfected with 3 weeks of miR-221-3p inhibitor demonstrated a significant decrease in muscularization compared with untreated SU5416-hypoxia and scrambled control-treated SU5416-hypoxia (Fig. 4G–H). These results suggest that silence of miR-221-3p attenuates the development of PAH in rats.

3.4. miR-221-3p regulates AXIN2 activity in human PASMC

To investigate the molecular mechanisms by which miR-221-3p promotes PASMC proliferation, putative miR-221-3p targets were predicted using TargetScan that is one of target prediction programs. The results of miR-221-3p target prediction revealed that the 3′-UTR of AXIN2 mRNA contains a complementary site for the miR-221-3p (Fig. 5A). To determine whether AXIN2 is a direct target gene of miR-221-3p, the 3′-UTR of AXIN2 containing the miR-221-3p binding sites was subcloned into a downstream of the luciferase reporter gene in pGL3 promoter vector. pGL3 reporter vector subcloned with 3′-UTR of AXIN2 was co-transfected with miR-221-3p mimic into PASMC and then performed the luciferase activity. As shown in Fig. 5B, AXIN2-3′-UTR-Luc activity in cells cotransfected with pGL3 reporter vector (expressing miR-221-3p) was significantly decreased in comparison to cells cotransfected with a control vector (expressing NC only). To determine whether miR-221-3p directly interacts with the 3′-UTR of AXIN2, the wild type (WT) or mutant (Mut) miR-221-3p-AXIN2 response elements were cloned into the pGL3 plasmid downstream of the luciferase reporter, and cells were transfected with miR-221-3p-mimic and the AXIN2 3′-UTR vectors. As shown in Fig. 5C, the luciferase reporter activity of WT, but not Mut inversely correlated with the miR-221-3p expression level. Our previous study has shown that the expression of Axin2 was significantly decreased in the lung tissue and PASMC both from PAH patients and rat model [4]. To know whether AXIN2 works as the downstream molecular target of miR-221-3p, the AXIN2 level was analyzed by qRT-PCR (Fig. 5D). AXIN2 protein levels in PASMC transfected with miR-221-3p mimic or NC were measured by a cell-based enzyme-linked immunosorbent assay, normalized to cytochrome *c* and presented as mean ± SEM (Fig. 5E). Fig. 5F displays that the protein levels of AXIN2 was decreased by miR-221-3p-mimic after treated with miR-221-3p-mimic and NC in PASMC for 24 h. The mRNA level of AXIN2 in PASMC was found to be significantly increased by miR-221-3p-inhibitor as determined by qRT-PCR (Fig. 5G). The protein level of AXIN2 in PASMC had the same tendency toward mRNA (Fig. 5H).

3.5. Hypoxic regulation of β-catenin expression in PASMC is dependent upon miR-221-3p and AXIN2

Under physiologic conditions, free β-catenin is targeted for degradation by a multiprotein complex composed of APC, GSK3β, CK1,

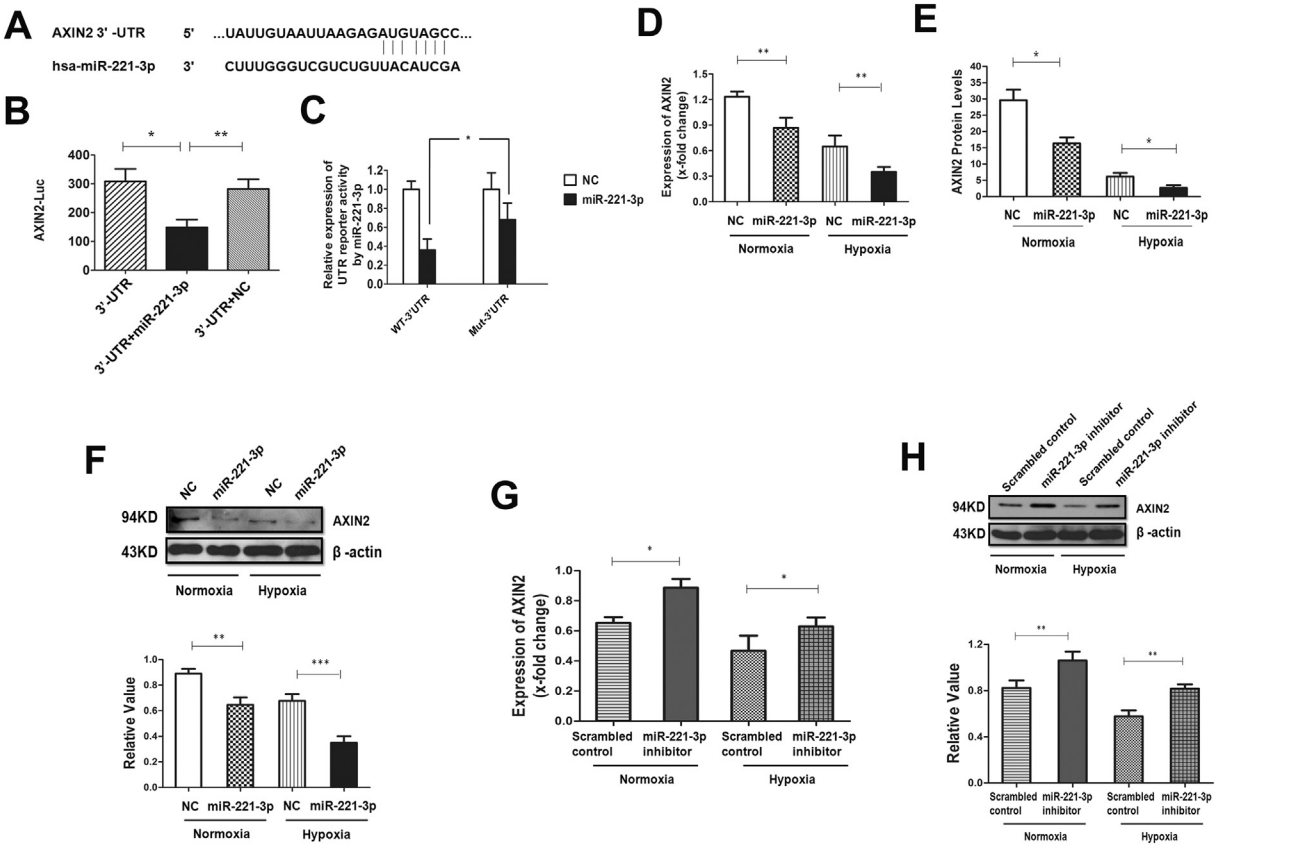

Fig. 5. Effects of miR-221-3p on AXIN2 expression.
A, Schematic representation of the miR-221-3p site in AXIN2 3′-UTR predicted by TargetScan. **B**, Luciferase reporter assay was conducted to verify that miR-221-3p directly bound to the 3′-UTR region of AXIN2 (n = 4). **C**, Luciferase activity was analyzed in PASMC co-transfected with miR-221-3p mimic or negative control with AXIN2 WT or Mut 3′-UTR reporter constructs (n = 4). **D**, The expression level of AXIN2 mRNA in PASMC transfected with miR-221-3p or NC mimic (n = 6). **E**, The expression level of AXIN2 protein in PASMC transfected with miR-221-3p or NC mimic were measured by a cell-based enzyme-linked immunosorbent assay, normalized to cytochrome *c* (n = 4). **F**, The expression level of AXIN2 protein in PASMC transfected with miR-221-3p or NC mimic under normoxia or hypoxia (n = 4). **G**, The expression level of AXIN2 mRNA in PASMC transfected with miR-221-3p inhibitor or scrambled control under normoxia or hypoxia (n = 6). **H**, The expression level of AXIN2 protein in PASMC transfected with miR-221-3p inhibitor under normoxia or hypoxia (n = 4). *p < 0.05, **p < 0.01, ***p < 0.001 compared to NC control or scrambled control. Bars indicate mean ± SEM. miR-221-3p, microRNA-221-3p; PASMC, pulmonary artery smooth muscle cells; NC, negative oligonucleotide; qPCR, real-time quantitative PCR; AXIN2, axis inhibition protein 2.

and either AXIN1 or AXIN2 [32]. AXIN2 inhibition by hypoxia has been identified by our recent study as a key event for vascular remodeling by stimulating angiogenesis via regulating β-catenin at the transcriptional level [4]. We first measured β-catenin expression in PASMC in response to hypoxia by qPCR and western blot analysis. Fig. 6A shows that β-catenin mRNA expression was significantly up-regulated by hypoxia in a time-dependent manner. Western blot and densitometric analysis confirmed that β-catenin protein expression was also significantly induced by hypoxia (Fig. 6B–C). We then determined whether treatment of PASMC with miR-221-3p mimic induced mRNA and protein expression level of β-catenin. Fig. 6D–F shows that the mRNA and protein expression of β-catenin was significantly up-regulated at 24 h by miR-221-3p mimic treatment. Further analysis indicated that mRNA and protein expression of β-catenin was significantly up-regulated by siAXIN2 (Fig. 6G–I). Immunocytochemistry further demonstrating the decreased Axin2 and increased β-catenin expression in hypoxic PASMC (green color represents β-catenin, red color represents Axin2), which were reversed by miR-221-3p inhibitor (Fig. 6J). Negative controls in each experiment with either serum or secondary antibody alone showed no immunofluorescence (data not shown). The results were consistent with our recently reports, which has reported that β-catenin was up-regulated in lung tissue of PAH patients and AXIN2 KO mice [4].

3.6. miR-221-3p promotes the proliferation of PASMC and its effects are attenuated by AXIN2 over-expression or β-catenin inhibition

To confirm that these cellular changes induced by miR-221-3p were mediated by AXIN2, we examined the impact of AXIN2 over-expression on the efficacy of miR-221-3p mimic. Over-expression of AXIN2 substantially reduced the viability of PASMC induced by miR-221-3p mimic (Fig. 7A). Inhibition of β-catenin by a small molecule inhibitor-XAV-939 repressed PASMC proliferation induced by miR-221-3p mimic, demonstrating that β-catenin is involved in the proliferation of PASMC mediated by miR-221-3p (Fig. 7B). Moreover, over-expression of β-catenin substantially reversed the decreased viability of PASMC by miR-221-3p inhibitor (Fig. 7C). The role of AXIN2 or β-catenin on the pro-proliferative effects of miR-221-3p on PASMC was investigated by BrdU assay (Fig. 7D–E). We also investigated the effects of over-expressed β-catenin on decreased PASMC proliferation by miR-221-3p inhibitor (Fig. 7F). The mRNA expression of PCNA, cyclin A, cyclin D and cyclin E was up-regulated by miR-221-3p, and the pro-proliferative effects of miR-221-3p were reversed after either over-expressed AXIN2 or inhibition of β-catenin with XAV-939. These results indicate that miR-221-3p promotes the proliferation of PASMC by regulating the expression of cell cycle proteins to advance cell cycle progression via AXIN2 and β-catenin signaling pathway (Fig. 7G–H).

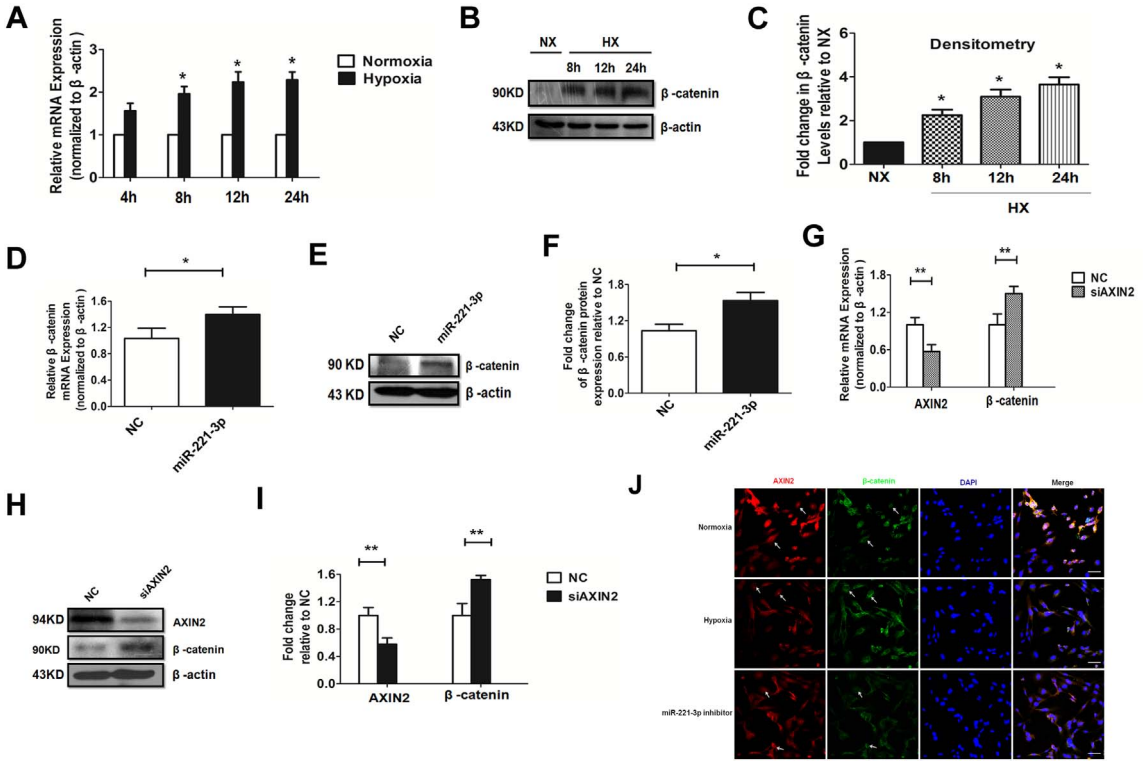

Fig. 6. Role of miR-221-3p in controlling β-catenin expression in PASMC.
A, The expression level of β-catenin mRNA in PASMC under normoxia (NX) or hypoxia (HX) (n = 4). **B**, β-catenin protein level was determined using Western blot in PASMC under normoxia or hypoxia. **C**, Densitometric analysis of multiple blots from experiment in **B** (n = 5). **D**, The expression level of β-catenin mRNA in PASMC transfected with NC or miR-221-3p mimic (n = 5). **E**, Western blot was used to verify the expression of β-catenin in PASMC transfected with NC or miR-221-3p mimic. **F**, Densitometric analysis of multiple blots from experiment described in **E** (n = 6). **G**, Expression fold changes of AXIN2 and β-catenin mRNA in PASMC transfected with AXIN2 siRNA (n = 6). **H**, Western blot analysis of β-catenin expression in PASMC transfected with siAXIN2 or NC. **I**, Densitometric analysis of multiple blots from experiment described in **H** (n = 6). **J**, The expression level of AXIN2 and β-catenin was determined in PASMC transfected with scrambled control or miR-221-3p inhibitor by immunofluorescence assays. Scale bars are 50 μm. *p < 0.05, **p < 0.01 compared to control. Bars indicate mean ± SEM. miR-221-3p, microRNA-221-3p; PASMC, pulmonary artery smooth muscle cells; siAXIN2, small interfering RNA against AXIN2; NC, negative oligonucleotide; NX, normoxia; HX, hypoxia.

3.7. The inhibitory effects of miR-221-3p inhibitor on PAH in rats were reversed by silencing the AXIN2 expression with siRNA

To investigate the effects of miR-221-3p on PAH, SU-5416/hypoxia rats were treated weekly with miR-221-3p inhibitor or siAXIN2 lentivirus for 3 weeks. RVSP and the weight ratio of RV to LV plus S were calculated. As shown in Fig. 8, increased RVSP and RV/(LV + S) in SU-5416/hypoxia-PAH rats was inhibited by miR-221-3p inhibitor. However, siAXIN2 treatments reversed the effects of miR-221-3p inhibitor. The results suggested miR-221-3p could improve PAH might via AXIN2.

4. Discussion

PAH is a vascular disease characterized by constricted and remodeled pulmonary arteries. This phenomenon is associated with enhanced proliferation and suppressed apoptosis of PASMC, and several other features that are considered as hallmarks of cancer. Since tumor suppressors and miRNAs are the major regulators of signaling in the cancer phenotype, we studied if the same type of regulation is operative in PAH [33]. Our previous studies have shown that PAH develops in AXIN2 (a tumor suppressor)-deficient mice. We hypothesized that the induction of miRNAs might lead to down-regulation of AXIN2 thus contribute to PAH [34]. Some of the differentially expressed miRNAs are known to be involved in idiopathic pulmonary fibrosis (IPF) and PAH [35]. Especially, miR-221-3p, the most up-regulated miRNA, is known to attenuate the toxic effects associated with lipopolysaccharide (LPS) stimulation [36]. MicroRNA-221 has been shown to play an oncogenic role in various types of cancer by targeting tumor suppressor genes, including PTEN, p27kip1, p57kip2, and PUMA [37–39]. A variety of studies manifested that miR-221-3p is involved in the regulation of vascular function [40]. In this study, we revealed the important role of miR-221-3p in promoting proliferation and migration of PASMC and provided a potential therapeutic target for human PAH. Elevated miR-221-3p expression was present in the lung tissue and PASMC from patients with PAH (Fig. 1A). These data are supported by findings from an experimental model of PAH, in which showed higher expression of miR-221-3p in lung tissue and PASMC as compared to control rats (Fig. 1C). However, the levels of miR-221-3p were lower among PAEC from PAH patients than that among PASMC (Fig. 1D). In addition, we detected the levels of miR-221-3p upon hypoxia using a qRT-PCR procedure in PASMC (Fig. 1E). miR-221-3p promoted proliferation and migration of human PASMC in vitro (Figs. 2–3). We also found that miR-221-3p inhibitor decreased the mRNA and protein expression of PCNA, cyclinA, cyclinD and cyclinE in PASMC (Fig. 2F–K). Inhibition of miR-221-3p in PAH rats by endotracheal drip normalized the RVSP and pulmonary vascular remodeling to levels close to those found in control rats, implicating the increased miR-221-3p as one mechanism necessary for the evolution of the PAH (Fig. 4). Our results were consistent with recently reports, which showed that ectopic expression of miR-221-3p induced primary tumor growth and lung metastasis in basal breast cancers.

To elucidate the mechanism of miR-221-3p on regulating PASMC proliferation, its target genes were investigated using bioinformatics software (TargetScan). We confirmed that AXIN2 is a direct target gene of miR-221-3p in PASMC by luciferase reporter assay, qRT-PCR and western blot (Fig. 5). Consistent with our previous findings, we also found that β-catenin expression was up-regulated in PASMC exposed to hypoxia, and its mRNA expression was increased correlated with miR-

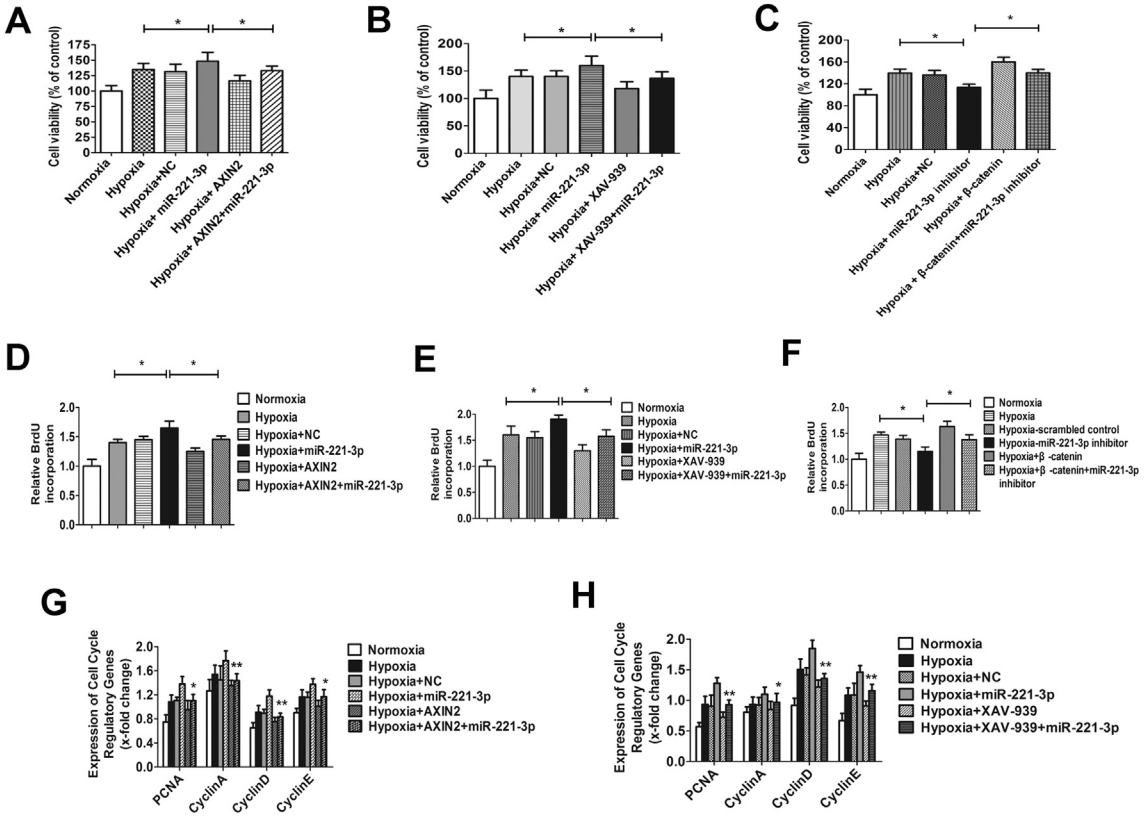

Fig. 7. Over-expression of AXIN2 or inhibition of β-catenin abolished miRNA-221-3p-induced proliferation of PASMC.
A, Cell viability assay was explored the effect of miR-221-3p expression alteration on cell proliferation. The rescue experiments for miR-221-3p overexpression were performed by ectopic expression of AXIN2 (n = 4). **B**, The rescue experiments for miR-221-3p overexpression was performed by downregulation of β-catenin with inhibitor-XAV-939 in PASMC (n = 4). **C**, Similar rescue experiments for miR-221-3p silencing was performed by upregulation of β-catenin in PASMC (n = 3). **D**, Rescue of miR-221-3p-induced proliferation in PASMC by AXIN2 upregulation using BrdU assay (n = 6). **E**, Rescue of miR-221-3p-induced proliferation in PASMC by β-catenin inhibitor-XAV-939 (n = 6). **F**, Rescue of miR-221-3p deficiency-induced suppressed cell proliferation by upregulation of β-catenin in PASMC (n = 6). **G**, Rescue of miR-221-3p-induced upregulation of PCNA, cyclin A, cyclin D and cyclin E in PASMC by AXIN2 upregulation (n = 4). **H**, Rescue of miR-221-3p-induced upregulation of PCNA, cyclin A, cyclin D and cyclin E in PASMC by XAV-939 (n = 4). *p < 0.05, **p < 0.01 compared to NC control or scrambled control. Bars indicate mean ± SEM. miR-221-3p, microRNA-221-3p; NC, negative oligonucleotide; PASMC, human pulmonary artery smooth muscle cells; PCNA, proliferating cell nuclear antigen.

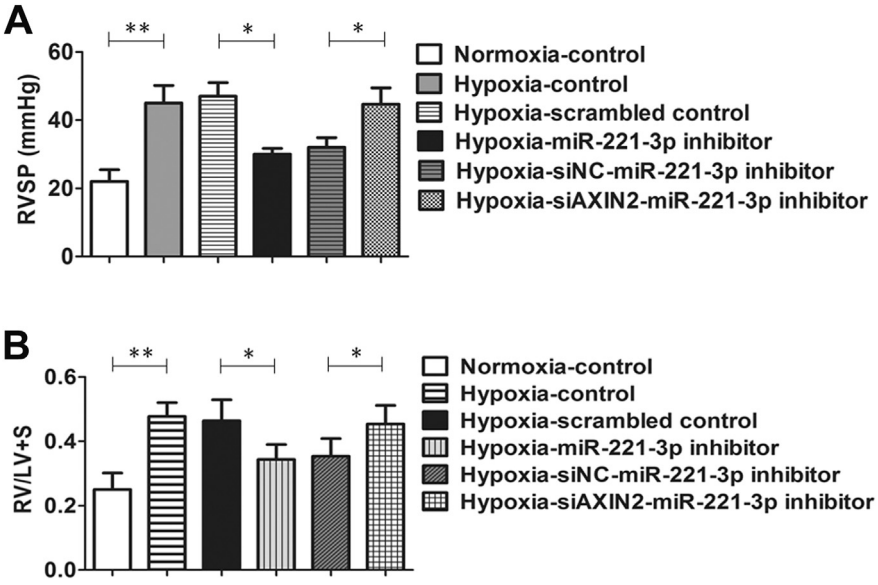

Fig. 8. AXIN2 silencing abolished the inhibitory effects of miR-221-3p inhibitor on PAH.
A, RVSP of muscularized peripheral arteries were determined. The relieving effect of miR-221-3p inhibitor on RVSP was rescued by injection of siAXIN2 lentivirus. **B**, Fulton index: RV/LV + S of muscularized peripheral arteries were determined. The relieving effect of miR-221-3p inhibitor on RV/LV + S was rescued by injection of siAXIN2 lentivirus. *p < 0.05, **p < 0.01 compared to NC control or scrambled control. Bars indicate mean ± SEM.

221-3p expression in PASMC (Fig. 6A–F). A computational approach identified AXIN2, which interferes with the DNA-binding activity of β-catenin, to contain a potential binding site for miR-221-3p. AXIN2 knockdown in PASMC increased the expression of β-catenin at both the mRNA and protein levels (Fig. 6G–I). Of note, over-expression of AXIN2 expression or down-regulation of β-catenin inhibited PASMC proliferation, yielding very much similar effect as that of miR-221-3p inhibitor. These results suggested that miR-221-3p exerted it pro-proliferative role in PASMC, at least in part, by targeting AXIN2 (Fig. 7A–F). Although genetic knockdown of miR-221-3p significantly

attenuated the development of PAH under the experimental conditions, AXIN2 over-expression could reverse it (Fig. 8A–B). However, our data are limited by the scarcity of data on pharmacological inhibition of miR-221-3p which precludes conclusions on the clinical relevance.

Recent publication has demonstrated that AXIN2 expression was significantly up-regulated in lung tissue derived from patients with idiopathic PAH [40]. This seems to contradict our results that AXIN2 expression level was decreased in both mice exposed to chronic hypoxia and patients with hypoxic PAH in remodeled pulmonary arterioles [4]. AXIN2 is a negative regulator of Wnt/β-catenin signaling by promoting the degradation of β-catenin in the proteasome. However, activation of Wnt/β-catenin through T-cell-specific transcription factor/lymphoid enhancer binding factor (TCF/LEF) sites induces the transcription of AXIN2 [41]. In our study, Axin2 mRNA was up-regulated by miR-221-3p inhibitor. This pattern of AXIN2 expression is consistent with the role of this protein in maintaining the cytosolic β-catenin at a steady state by a negative feedback mechanism. The enhanced proliferation of PASMC by miR-221-3p as early as 24 h in this study is likely related with the decrease in Axin2 expression. These findings suggest an association of AXIN2 in lung tissue from PAH patients with a variable presentation among different subtypes of disease. However, it is still unclear how this protein regulates these processes. The mechanisms may be related to the response to hypoxia stress that needs to be further exploited.

In PAEC examined, we did not detect a significant up-regulation of miR-221-3p expression upon hypoxia (**Fig. S3B**), implying a differential regulation of miR-221-3p in these two cell types. These findings are not completely explained, but paradoxical reactions of the PASMC in response to hypoxia as compared to PAEC may be a major reason [42]. miR-221-3p has no obvious effects on PAEC proliferation and cell cycle (**Fig. S3D and E**). Conversely, a recent study has described that miR-221-3p is primarily expressed in human aortic endothelial cells and it is shown that miR-221 affects aortic endothelial cells proliferation and apoptosis [40]. These controversial findings are not fully explained, but paradoxical reactions of the pulmonary vessels in response to hypoxia as compared to systemic vessels are a well-known phenomenon. Previous studies also revealed the differences in the cell type-specific response to hypoxia among genes between HAECs and HPAECs [43]. Our study may provide further evidence to understand the characteristics of the responses to hypoxia in the pulmonary circulation relative to systemic circulation. Depending on the type and context of different cells, the miR-221 family has been implicated in several mechanisms including cell growth, differentiation, and apoptosis. In our experiments, the differential effects of miR-221-3p on endothelial and smooth muscle cells are a novel observation. The mechanisms of these effects are unclear but might be explained by the different behavior of miR-221-3p upon oxygen deprivation in these cells.

Accumulating evidence suggests that aberrant activation of the β-catenin pathway plays a central role in the destruction of PASMC proliferation in PAH patients. For example, silencing AXIN2, a key component of the 'destruction complex', leads to nuclear β-catenin accumulation [44]. Our group previously described AXIN2-mediated regulation of β-catenin in PASMC. In our present study, the increased levels of miR-221-3p were associated with reduced expression of AXIN2, as such, highlight the relevance of the identified pathway in vivo. Association of β-catenin with several other factors has been well documented, although the functional significance of these interactions was not well defined. We showed the interaction between AXIN2 and β-catenin promoted regulation of miR-221-3p on PASMC proliferation. The detailed mechanism promoting this interaction is not known, but our previous studies suggest that they have mutual influence on the process of PAH regulated by miR-221-3p. Glycogen synthase kinase 3β (GSK3β) plays a central role in Wnt signaling as it is critical in stabilizing β-catenin in the cytoplasm. Independent of changes in nuclear GSK3β activity, AXIN2-GSK3β binding interactions can alter the ability of kinase to recognize and phosphorylate target substrates. Whereas GSK3β catalyzes β-catenin phosphorylation when both components are incorporated into an APC/Axin docking complex, alternate targets [45]. Recent study has showed that human miR-1246 promotes drug resistance, tumorigencity, and metastasis, by activation of the Wnt/β-catenin pathway through suppressing the expression of AXIN2 and GSK3β [46]. Our findings provide evidence for a cause-effect relationship between these pathways, but the evidence of how deregulation of AXIN2 by miR-221-3p affects the activity of β-catenin degradation complex still need future investigation.

5. Conclusions

This is the first study to provide mechanistic evidence for the implication of miR-221-3p up-regulation and the resulting reduction of AXIN2 and activation of β-catenin in the etiology of human PAH. miR-221-3p significantly promoted the proliferation of PASMC. In that sense, miR-221-3p may be one of the factors contributing to the PAH progress. Moreover, miR-221-3p inhibitor attenuated pulmonary vascular remodeling in PAH rats. These findings may have significant clinical implications and prognostic significance in patients with pre-existing pulmonary hypertension. Therefore, we describe miR-221-3p as a novel and specific therapeutic target and potential bio-marker for PAH.

Conflicts of interest

None.

Sources of funding

The study is supported by funds from the National Natural Science Foundation of China (81500039), Natural Science Foundation of Jiangsu Province (BK20160196), Project of Jiangsu Provincial Commission of Health and Family Planning (Nos. QNRC2016198), Science and Technology Agency of Jiangsu Province (BM2012108).

Acknowledgments

None.

Appendix A. Supplementary data

Supplementary data to this article can be found online at http://dx.doi.org/10.1016/j.vph.2017.07.002.

References

[1] S.L. Archer, G. Marsboom, G.H. Kim, H.J. Zhang, P.T. Toth, E.C. Svensson, J.R. Dyck, M. Gomberg-Maitland, B. Thebaud, A.N. Husain, N. Cipriani, J. Rehman, Circulation 121 (2010) 2661.
[2] A.M. Rothman, N.D. Arnold, J.A. Pickworth, J. Iremonger, L. Ciuclan, R. Allen, S. Guth-Gundel, M. Southwood, N.W. Morrell, M. Thomas, S.E. Francis, D.J. Rowlands, A. Lawrie, J. Clin. Invest. 126 (2016) 2495.
[3] J. Meloche, M. Le Guen, F. Potus, J. Vinck, B. Ranchoux, I. Johnson, F. Antigny, E. Tremblay, S. Breuils-Bonnet, F. Perros, S. Provencher, S. Bonnet, Am. J. Phys. Cell Physiol. 309 (2015) C363.
[4] X. Nie, G. Qin, W. Mao, W. Wang, Y. Chang, D. Wei, M. Zhou, B. Wu, J. Chen, J. Hypertens. 34 (2016) 877.
[5] E.M. Small, E.N. Olson, Nature 469 (2011) 336.
[6] L. Deng, F.J. Blanco, H. Stevens, R. Lu, A. Caudrillier, M. McBride, J.D. McClure, J. Grant, M. Thomas, M. Frid, K. Stenmark, K. White, A.G. Seto, N.W. Morrell, A.C. Bradshaw, M.R. MacLean, A.H. Baker, Circ. Res. 117 (2015) 870.
[7] L. Pitzler, M. Auler, K. Probst, C. Frie, V. Bergmeier, T. Holzer, D. Belluoccio, J. van den Bergen, J. Etich, H. Ehlen, Z. Zhou, W. Bielke, E. Poschl, M. Paulsson, B. Brachvogel, Stem Cells 34 (2016) 1297 (Dayton, Ohio).
[8] C.X. Huang, N. Chen, X.J. Wu, C.H. Huang, Y. He, R. Tang, W.M. Wang, H.L. Wang, FASEB J. 29 (2015) 4901.
[9] S. Rajasekaran, P. Rajaguru, P.S. Sudhakar Gandhi, Front. Pharmacol. 6 (2015) 254.
[10] A. Kuehbacher, C. Urbich, S. Dimmeler, Trends Pharmacol. Sci. 29 (2008) 12.
[11] X.W. Wang, X.J. He, K.C. Lee, C. Huang, J.B. Hu, R. Zhou, X.Y. Xiang, B. Feng, Z.Q. Lu, Int. J. Cardiol. 208 (2016) 79.

[12] X. Liu, Y. Cheng, S. Zhang, Y. Lin, J. Yang, C. Zhang, Circ. Res. 104 (2009) 476.
[13] W. Mao, W. Xia, J. Chen, Chest 145 (2014) 192.
[14] S.M. Bhorade, A.N. Husain, C. Liao, L.C. Li, V.N. Ahya, M.A. Baz, V.G. Valentine, R.B. Love, H. Seethamraju, C.G. Alex, R. Bag, N.C. DeOliveira, W.T. Vigneswaran, E.R. Garrity, S.M. Arcasoy, Chest 143 (2013) 1717.
[15] J.W. Barnes, L. Tian, G.A. Heresi, C.F. Farver, K. Asosingh, S.A. Comhair, K.S. Aulak, R.A. Dweik, Circulation 131 (2015) 1260.
[16] M. Zungu-Edmondson, N.V. Shults, C.M. Wong, Y.J. Suzuki, Cardiovasc. Res. 110 (2016) 30.
[17] D. Farkas, A.A. Alhussaini, D. Kraskauskas, V. Kraskauskiene, C.D. Cool, M.R. Nicolls, R. Natarajan, L. Farkas, Am. J. Respir. Cell Mol. Biol. 51 (2014) 413.
[18] A.L. Zaiman, R. Damico, A. Thoms-Chesley, D.C. Files, P. Kesari, L. Johnston, M. Swaim, S. Mozammel, A.C. Myers, M. Halushka, H. El-Haddad, L.A. Shimoda, C.F. Peng, P.M. Hassoun, H.C. Champion, R.N. Kitsis, M.T. Crow, Circulation 124 (2011) 2533.
[19] R.P. Heilman, M.B. Lagoski, K.J. Lee, J.M. Taylor, G.A. Kim, S.K. Berkelhamer, R.H. Steinhorn, K.N. Farrow, Am. J. Physiol. Heart Circ. Physiol. 308 (2015) H1575.
[20] R. Savai, H.M. Al-Tamari, D. Sedding, B. Kojonazarov, C. Muecke, R. Teske, M.R. Capecchi, N. Weissmann, F. Grimminger, W. Seeger, R.T. Schermuly, S.S. Pullamsetti, Nat. Med. 20 (2014) 1289.
[21] J. Feng, Y. Liu, N. Dobrilovic, L.M. Chu, C. Bianchi, A.K. Singh, F.W. Sellke, Circulation 128 (2013) S144.
[22] Y. Song, J.E. Jones, H. Beppu, J.F. Keaney Jr., J. Loscalzo, Y.Y. Zhang, Circulation 112 (2005) 553.
[23] B. Icli, A.K. Wara, J. Moslehi, X. Sun, E. Plovie, M. Cahill, J.F. Marchini, A. Schissler, R.F. Padera, J. Shi, H.W. Cheng, S. Raghuram, Z. Arany, R. Liao, K. Croce, C. MacRae, M.W. Feinberg, Circ. Res. 113 (2013) 1231.
[24] J. Li, S. Yang, W. Yan, J. Yang, Y.J. Qin, X.L. Lin, R.Y. Xie, S.C. Wang, W. Jin, F. Gao, J.W. Shi, W.T. Zhao, J.S. Jia, H.F. Shen, J.R. Ke, B. Liu, Y.Q. Zhao, W.H. Huang, K.T. Yao, D.J. Li, D. Xiao, Lab. Investig. 95 (2015) 1056.
[25] T.C. Foster, A. Rani, A. Kumar, L. Cui, S.L. Semple-Rowland, Mol. Ther. 16 (2008) 1587.
[26] T.O. Yau, C.W. Wu, Y. Dong, C.M. Tang, S.S. Ng, F.K. Chan, J.J. Sung, J. Yu, Br. J. Cancer 111 (2014) (1765).
[27] M.F. Smith Jr., J. Novotny, V.S. Carl, L.D. Comeau, Glycobiology 16 (2006) 221.
[28] H.K. Park, E.C. Park, S.W. Bae, M.Y. Park, S.W. Kim, H.S. Yoo, M. Tudev, Y.H. Ko, Y.H. Choi, S. Kim, D.I. Kim, Y.W. Kim, B.B. Lee, J.B. Yoon, J.E. Park, Circulation 114 (2006) 886.
[29] K. Satoh, T. Satoh, N. Kikuchi, J. Omura, R. Kurosawa, K. Suzuki, K. Sugimura, T. Aoki, K. Nochioka, S. Tatebe, S. Miyamichi-Yamamoto, M. Miura, T. Shimizu, S. Ikeda, N. Yaoita, Y. Fukumoto, T. Minami, S. Miyata, K. Nakamura, H. Ito, K. Kadomatsu, H. Shimokawa, Circ. Res. 115 (2014) 738.
[30] W. Wang, P. Chen, M. Tang, J. Li, Y. Pei, S. Cai, X. Zhou, S. Chen, Am. J. Transl. Res. 7 (2015) 1332.
[31] C. Sinha, A. Ren, K. Arora, C.S. Moon, S. Yarlagadda, W. Zhang, S.B. Cheepala, J.D. Schuetz, A.P. Naren, J. Biol. Chem. 288 (2013) 3786.
[32] K. Brauburger, S. Akyildiz, J.G. Ruppert, M. Graeb, D.B. Bernkopf, M.V. Hadjihannas, J. Behrens, FEBS J. 281 (2014) 787.
[33] R. Paulin, A. Courboulin, M. Barrier, S. Bonnet, J. Mol. Med. 89 (2011) 1089 (Berlin, Germany).
[34] A.P. Wang, X.H. Li, S.X. Gong, W.Q. Li, C.P. Hu, Z. Zhang, Y.J. Li, Eur. J. Pharmacol. 765 (2015) 565.
[35] S. Sharma, S. Umar, F. Potus, A. Iorga, G. Wong, D. Meriwether, S. Breuils-Bonnet, D. Mai, K. Navab, D. Ross, M. Navab, S. Provencher, A.M. Fogelman, S. Bonnet, S.T. Reddy, M. Eghbali, Circulation 130 (2014) 776.
[36] J. Zhang, S.L. Fu, Y. Liu, Y.L. Liu, W.J. Wang, Int. J. Mol. Sci. 16 (2015) 22438.
[37] S. Sarkar, H. Dubaybo, S. Ali, P. Goncalves, S.L. Kollepara, S. Sethi, P.A. Philip, Y. Li, Am. J. Cancer Res. 3 (2013) 465.
[38] C. le Sage, R. Nagel, D.A. Egan, M. Schrier, E. Mesman, A. Mangiola, C. Anile, G. Maira, N. Mercatelli, S.A. Ciafre, M.G. Farace, R. Agami, EMBO J. 26 (2007) 3699.
[39] J. Shi, Y. Zhang, N. Jin, Y. Li, S. Wu, L. Xu, Oncol. Res. 25 (2017) 523.
[40] Y. Xue, Z. Wei, H. Ding, Q. Wang, Z. Zhou, S. Zheng, Y. Zhang, D. Hou, Y. Liu, K. Zen, C.Y. Zhang, J. Li, D. Wang, X. Jiang, Atherosclerosis 241 (2015) 671.
[41] K. Bhukhai, K. Suksen, N. Bhummaphan, K. Janjorn, N. Thongon, D. Tantikanlayaporn, P. Piyachaturawat, A. Suksamrarn, A. Chairoungdua, J. Biol. Chem. 287 (2012) 36168.
[42] N. Bettaga, R. Jager, S. Dunnes, D. Groneberg, A. Friebe, Angiogenesis 18 (2015) 245.
[43] D.G. Peters, W. Ning, T.J. Chu, C.J. Li, A.M. Choi, Physiol. Genomics 26 (2006) 99.
[44] J.A. Hulin, T.D. Nguyen, S. Cui, S. Marri, R.T. Yu, M. Downes, R.M. Evans, H. Makarenkova, R. Meech, Stem Cells 34 (2016) 2169 (Dayton, Ohio).
[45] A.K. Olsen, M. Coskun, M. Bzorek, M.H. Kristensen, E.T. Danielsen, S. Jorgensen, J. Olsen, U. Engel, S. Holck, J.T. Troelsen, Carcinogenesis 34 (2013) 1361.
[46] S. Chai, K.Y. Ng, M. Tong, E.Y. Lau, T.K. Lee, K.W. Chan, Y.F. Yuan, T.T. Cheung, S.T. Cheung, X.Q. Wang, N. Wong, C.M. Lo, K. Man, X.Y. Guan, S. Ma, Hepatology 64 (2016) 2062 (Baltimore, Md.).